7146 J. Med. Chem. 2010, 53, 7146–7155
DOI: 10.1021/jm101144f

Journal of Medicinal Chemistry Article

Discovery of 1-(4-(4-Propionylpiperazin-1-yl)-3-(trifluoromethyl)phenyl)-9-(quinolin-3-yl)benzo[h][1,6]naphthyridin-2(1*H*)-one as a Highly Potent, Selective Mammalian Target of Rapamycin (mTOR) Inhibitor for the Treatment of Cancer

Qingsong Liu,[†,‡] Jae Won Chang,[†,‡] Jinhua Wang,[†,‡] Seong A. Kang,[§] Carson C. Thoreen,[†,‡] Andrew Markhard,[§] Wooyoung Hur,[†,‡] Jianming Zhang,[†,‡] Taebo Sim,[†,‡] David M. Sabatini,[§,∥,⊥] and Nathanael S. Gray*[,†,‡]

[†]*Department of Cancer Biology, Dana Farber Cancer Institute, 44 Binney Street, Boston, Massachusetts 02115,* [‡]*Department of Biological Chemistry and Molecular Pharmacology, Harvard Medical School, 250 Longwood Avenue, Boston, Massachusetts 02115,* [§]*Whitehead Institute for Biomedical Research, 9 Cambridge Center, Cambridge, Massachusetts 02142,* [∥]*Howard Hughes Medical Institute, Department of Biology, Massachusetts Institute of Technology, Cambridge, Massachusetts 02139, and* [⊥]*Koch Center for Integrative Cancer Research at MIT, 77 Massachusetts Avenue, Cambridge, Massachusetts 02139*

Received June 27, 2010

The mTOR protein is a master regulator of cell growth and proliferation, and inhibitors of its kinase activity have the potential to become new class of anticancer drugs. Starting from quinoline **1**, which was identified in a biochemical mTOR assay, we developed a tricyclic benzonaphthyridinone inhibitor **37** (Torin1), which inhibited phosphorylation of mTORC1 and mTORC2 substrates in cells at concentrations of 2 and 10 nM, respectively. Moreover, Torin1 exhibits 1000-fold selectivity for mTOR over PI3K (EC_{50} = 1800 nM) and exhibits 100-fold binding selectivity relative to 450 other protein kinases. Torin1 was efficacious at a dose of 20 mg/kg in a U87MG xenograft model and demonstrated good pharmacodynamic inhibition of downstream effectors of mTOR in tumor and peripheral tissues. These results demonstrate that Torin1 is a useful probe of mTOR-dependent phenomena and that benzonaphthridinones represent a promising scaffold for the further development of mTOR-specific inhibitors with the potential for clinical utility.

Introduction

The mammalian target of rapamycin (mTOR[a]) is a key node in the PI3K/Akt/mTOR signaling pathway that is often deregulated in human cancer.[1] In conjunction with PI3K and Akt/PKB, mTOR integrates signals derived from extracellular cues, such as growth factors, energy, stress, and nutrients, and regulates growth-related cellular processes, including mRNA translation, ribosome biogenesis, autophagy, and metabolism. The mTOR serine/threonine protein kinase shares a structurally similar catalytic domain with other PIKK family members, including PI3Ks, DNA-PK, ATM, ATR, and SMG-1.[2] mTOR exists in at least two distinct protein complexes in cells: mTOR complex 1 (mTORC1) and mTOR complex 2 (mTORC2). mTORC1 regulates mRNA translation through the phosphorylation of S6K1 and 4EBP1, while mTORC2 regulates cell survival through the phosphorylation of Akt/PKB and other AGC-family kinases, such as SGK. Hyperactivation of the mTOR signaling pathway is often implicated in cellular growth deregulation in cancer, and therefore there has been a substantial effort to develop mTOR inhibitors for potential clinical application.[3,4]

The development of ATP-competitive mTOR inhibitors was not viewed as a priority until recently because of rapamycin and its analogues (known as rapalogues), which were widely considered highly potent and selective allosteric inhibitors of mTORC1. In some cell types, rapamycin can also inhibit mTORC2.[5] Unfortunately, clinical success of these compounds has been limited to a small number of relatively rare cancers, including mantle cell lymphoma, renal cell carcinoma, and endometrial cancer.[6] Several explanations for this limited efficacy have been proposed: (1) rapamycin may only be effective in tumors where it is also capable of inhibiting mTORC2, (2) the induction by rapamycin of a feedback signal that leads to the hyperactivation of PI3K signaling might undermine the antiproliferative effect of mTORC1 inhibition, or (3) in many cell types, rapamycin fails to significantly inhibit mTORC1 kinase activity toward substrates, such as 4E-BP1, that are major regulators of proliferation.[7,8] It is currently unknown whether any or all of these explanations account for the apparently limited clinical efficacy of rapamycin and its derivatives. Nonetheless, these potential deficiencies in rapamycin-based therapies have spurred the rapid development of ATP-competitive mTOR inhibitors that target both mTOR complexes. Recently, a number of selective ATP-competitive mTOR inhibitors

*To whom correspondence should be addressed. Phone: 1-617-582-8590. Fax: 1-617-582-8615. E-mail: Nathanael_gray@dfci.harvard.edu

[a] Abbreviations: mTOR, mammalian target of rapamycin; Akt, v-akt murine thymoma viral oncogene homologue 1; ATP, adenosine triphosphate; PIKKs, PI3K related kinases; DNA-PK, DNA activated protein kinase; ATM, ataxia telangiectasia mutated kinase; ATR, ataxia telangiectasia and Rad-3-related kinase; SMG-1, serine/threonine protine kinase-1; 4EBP1, eukaryotic translation initiation factor 4E-binding protein 1; PK, pharmacokinetics; PD, pharmacodynamics; ADME, absorption, distribution, metabolism, excretion; MEFs, mouse embryo fibroblasts.

 Published on Web 09/22/2010

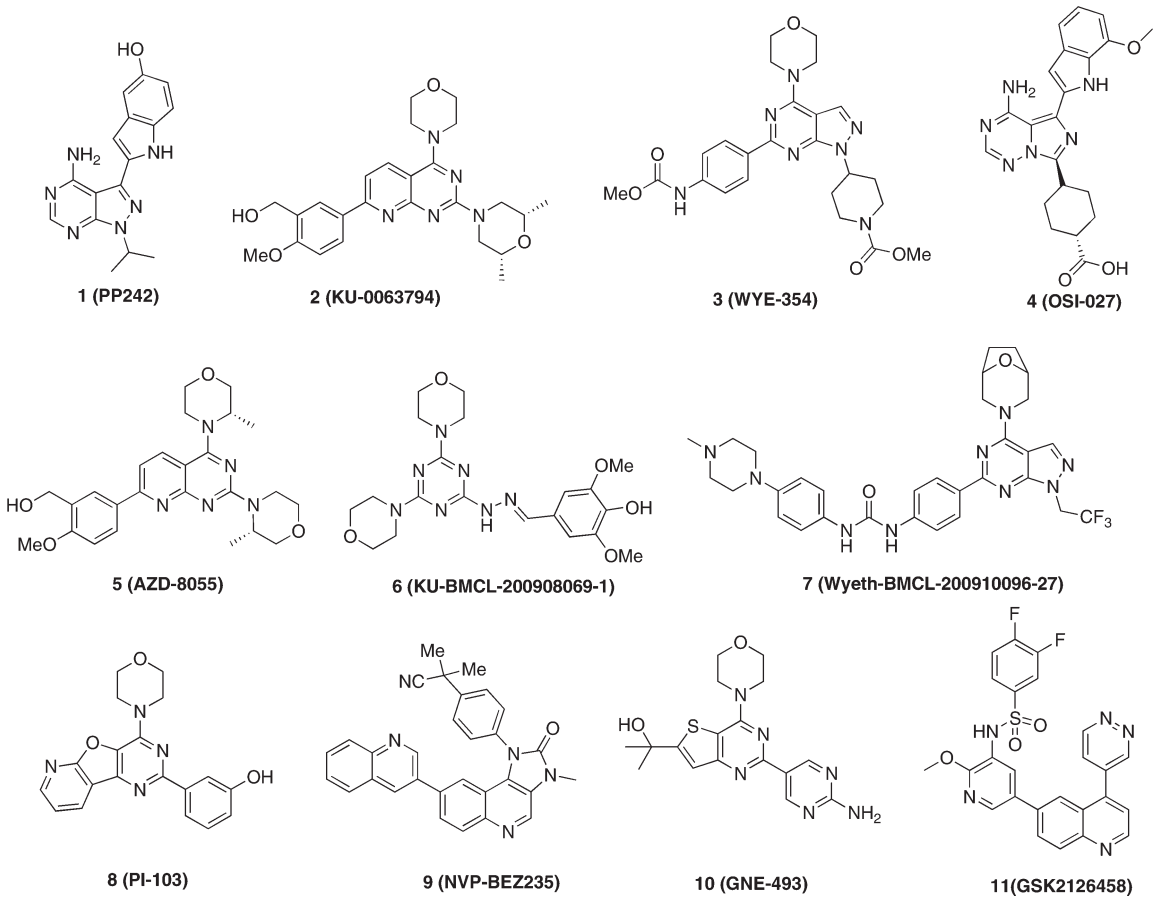

Figure 1. Chemical structures of reported ATP-competitive mTOR inhibitors.

have been reported, including **37** (Torin1),[7] **1** (PP242),[8] **2** (KU-0063794),[9] **3** (WYE-354),[10] **4** (OSI-027),[11] **5** (AZD-8055),[12] **6** (KU-BMCL-200908069-1),[13] and **7** (Wyeth-BMCL-200910096-27),[14] as well as a number of compounds that are capable of inhibiting both PI3K and mTOR and other PIKK-family kinases such as **8** (PI-103),[15] **9** (NVP-BEZ235),[16] **10** (GNE-493),[17] and **11** (GSK2126458)[18] (Figure 1). Here we describe our screening and medicinal chemistry efforts that resulted in the identification of benzonapthridinones exemplified by **37** as highly potent and selective mTOR inhibitors.

Results and Discussion

To identify compounds capable of inhibiting mTOR kinase activity, we established a medium-throughput biochemical assay utilizing purified mTORC1 from mammalian cells.[19] We screened a compound library consisting of both known kinase inhibitors as well as heterocycles that would be anticipated to have the propensity to bind to the ATP binding pocket of kinases.[20] This screening effort resulted in the identification of several classes of compounds; however, based on the criteria of the scaffold selectivity, we focused our attention on quinoline hit compound **12**. Although compound **12** exhibited only moderate biochemical inhibitory activity (mTORC1 IC_{50} = 5 μM) and was unable to inhibit phosphorylation of the cellular mTORC1 substrate S6K at a concentration of 10 μM, it did exhibit selectivity for PIKK-family kinases when screened in binding assays against a panel of approximately 400 kinases at a concentration of 10 μM (KinomeScan). In addition, the quinoline and isosteric quinazoline scaffolds are "privileged" ATP-site binders and several highly selective kinase inhibitors

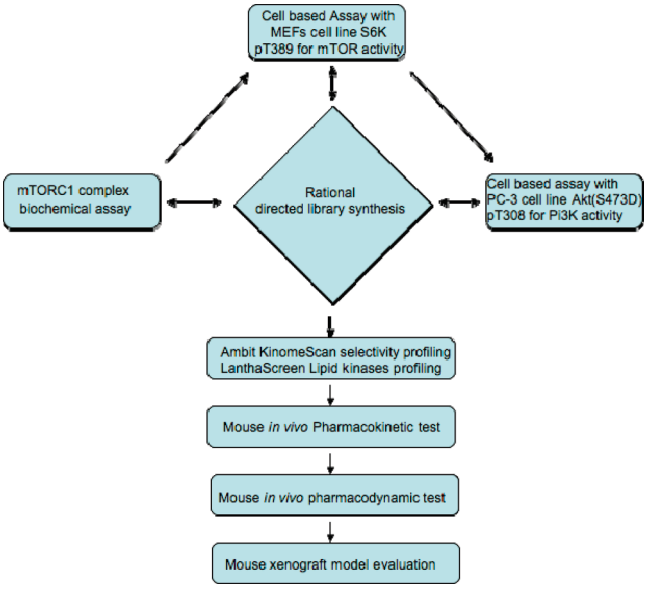

Figure 2. Screening flowchart for development of mTOR inhibitors.

such as HKI-272[21] and lapatinib[22] are built from these heterocyclic cores.

To optimize the cellular potency and selectivity of "hit" compound **12**, we established a streamlined flowchart of biochemical and cellular assays to explore the structure–activity relationship (Figure 2). Newly synthesized compounds were initially screened for their ability to inhibit mTORC1 activity by monitoring the inhibition of phosphorylation of

Scheme 1[a]

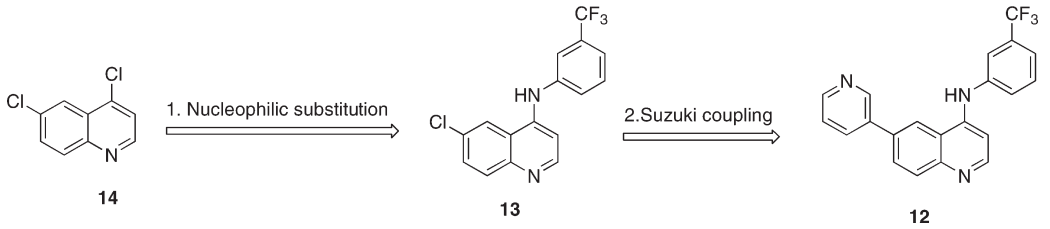

[a] Reagents and conditions: (1) appropriate aniline, 1,4-dioxane, 100 °C, 4−12 h; (2) appropriate boronic acid, $PdCl_2(Ph_3P)_2$, *t*-Bu-Xphos, Na_2CO_3, dioxane, 100 °C, 6 h.

Table 1. Enzymatic and Cellular Activities Profile of Acyclic Quinoline Series[a]

Entry	Structure	mTOR IC_{50}(nM) mTORC1	mTOR IC_{50}(nM) Cellular	PI3K IC_{50}(nM) Cellular
15	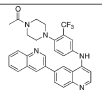	1700	>300	>300
16	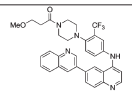	966	>300	>300
17	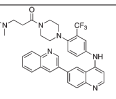	3810	>300	>300

[a] The IC_{50} determinations are the mean of two of independent measurement with standard error of <20%. For cellular assay, 300 nM was the highest concentration tested

T389 of S6K1 by immunoblot analyses in mouse embryonic fibroblasts (MEFs). The cellular assay was primarily used to prioritize compounds and, in parallel, compounds were also tested using an in vitro mTORC1 kinase assay. Compounds that exhibited promising cellular mTORC1 activity were assessed for selectivity versus inhibition of cellular PI3K activity by monitoring inhibition of Akt T308 in PC-3 cells that stably express the phosphomimetic S473D mutant of Akt.[7] The S473D mutant of Akt was used to achieve a more pure PI3K-dependent phosphorylation read-out by eliminating the effect of mTORC2 phosphorylation at that site, which normally facilitates phosphorylation at T308 by PDK1.[23] The most potent and selective candidates to emerge from this reiterative process between the chemical modification and biological evaluation were subject to broad kinase selectivity profiling using the Ambit KinomeScan and LifeTechnologies LanthaScreen platforms. Compounds that passed our criteria for triage were further profiled for their in vitro and in vivo drug metabolism and pharmacokinetic properties (DMPK) and finally tested in a U87MG tumor xenograft model.

To begin the SAR exploration of compound **12**, we generated a number of analogues by varying the side chains at 4- and 6-positions of the quinoline (Scheme 1). A few representative compounds that emerged from this effort are illustrated by compounds **15**, **16**, and **17** (Table 1). Unfortunately, these substitutions generally resulted in very minor changes in biochemical IC_{50} values and none of the compounds inhibited mTOR or PI3K activity in cellular assays at submicromolar concentrations (Table 1).

A substructure search of compound **12** identified a broad class of tricyclic quinoline-derived dual PI3K/mTOR inhibitors exemplified by **9** as containing a similar substructure[24,25] (Figure 1). Tricylic core structure have been exploited in the development of numerous other kinase inhibitors targeting EGFR,[26a] PDGFR,[26b] Aurora,[26c] CK2,[26d] and IKK.[26e] **9** was predicted to bind to PI3K using the quinoline nitrogen to form a key hydrogen bond to the kinase "hinge region".[25] The cyclic urea moiety was predicted to be important for constraining the pendant phenyl ring to the presumed bioactive conformation. We decided to introduce a similar constraint by introducing a six-membered lactam that would result in a tricyclic scaffold which would facilitate additional diversification points as well as introduce the potentially important carbonyl oxygen for the potency.

The introduction of this additional ring constraint resulted in benzonaphthridinone compound **18**, which exhibited a dramatic 1000-fold improved mTOR cellular potency compared to that of the screening hit compound **12**. Compound **18** possessed a biochemical IC_{50} of 5.4 nM against mTORC1 enzyme and an IC_{50} of 3 nM for inhibition of S6K phosphorylation in cells without any detectable inhibitory activity on PI3K up to a concentration of 300 nM (Table 2).

To rationalize the potency of **18** in a structural context, we docked compound **18** into the ATP-binding site of an mTOR homology model built using the related Pi3Kγ crystal structure (PDB code: 3DBS) (Figure 3). Similar to the published homology model of **9** with Pi3Kγ,[27] a hydrogen bond was predicted to form between the quinolione nitrogen of compound **18** and Val2240 within the kinase hinge region.[16] A comparison to the proposed binding mode of morpholine-derived mTOR inhibitors such as **8** suggests that the morpholine oxygen makes a similar hydrogen bond. The quinoline moiety of compound **18** was predicted to reside within the inner hydrophobic pocket formed by Glu2190, Leu2192, Asp2195, Tyr2225, Asp2357, Phe2358, Gly2359, and Asp2360. The phenyl piperazine side chain was oriented below a loop defined by residues from Ile2183 to Gln2187, which occupy a similar region of the ATP-binding site as the "P-loop" of protein kinases. Using this homology model as a guide, we embarked on a further elaboration of the benzonaphthridione scaffold at the quinoline (**R1**) and lactam phenyl (**R2**) positions. Previous efforts to optimize PI3K inhibitors have suggested that modification at either of these positions could modulate potency, while the **R1** position may provide a stronger contribution to specificity versus other PIKK-family kinases.[27] In addition, to improve the extremely poor water-solubility of this compound class, we continued our SAR exploration with **R2** fixed as a phenyl piperazine, which introduces a water solubility enhancing basic secondary nitrogen versus the acyl piperazine present in our library compounds (Figure 4). The target compounds were synthesized using a

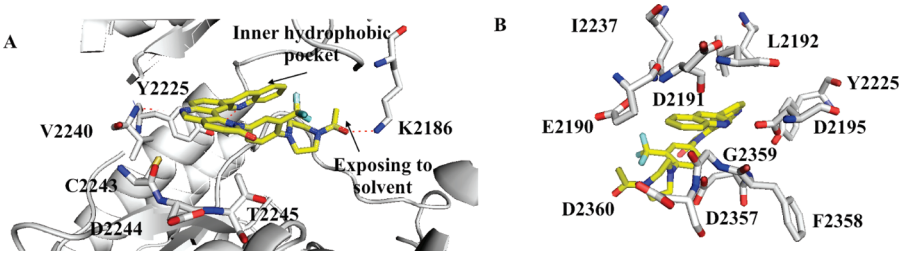

Figure 3. Model demonstration of compound **18** binding with mTOR.

Scheme 2[a]

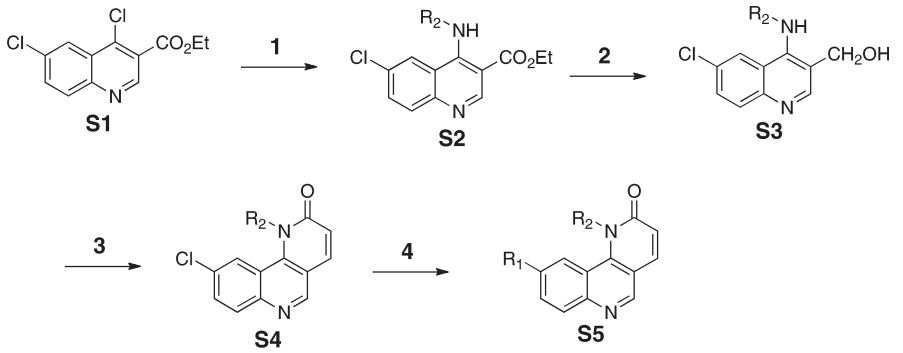

[a] Reagents and conditions: (1) aniline (R_2NH_2), 1,4-dioxane, 100 °C, 4 h; (2) LAH, THF, 0 °C−rt, 4 h; (3) (a) MnO_2, CH_2Cl_2, rt, 6 h, (b) triethyl phosphonoacetate, K_2CO_3, EtOH, 100 °C, 12 h; (4) $R_1B(OH)_2$, $PdCl_2(Ph_3P)_2$, *t*-Bu-Xphos, Na_2CO_3, 1,4-dioxane, 100 °C, 12 h.

Table 2. Enzymatic and Cellular Activities Profile of Compound **18**

Entry	Structure	mTOR IC_{50}(nM) mTORC1	mTOR IC_{50}(nM) Cellular	PI3K IC_{50}(nM) Cellular
18	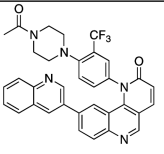	5.4	3	>300

four-step sequence starting from dichloroquinoline scaffold **S1** (Scheme 2). Introduction of substituted anilines in the first step was followed by construction of the six-membered lactam using a Horner−Wadsworth−Emmons reaction. The **R1** side chain was then introduced via palladium-mediated coupling with the desired boronic acid. The biological activities of the compounds that resulted from this effort are illustrated in Table 3 and 4.

Removal of the acyl group of compound **18** to yield compound **19** resulted in a 2−10-fold reduction in potency in both biochemical and cellular assays. On the basis of the homology model, this could be rationalized by the potential loss of a hydrogen bond between the amide carbonyl oxygen and epsilon amine of Lys2186. Removal of the quinoline nitrogen of compound **19** to yield compound **25** resulted in more than a 10-fold loss in cellular mTOR potency, which may be attributable to the loss of a hydrogen bond between the quinoline N and the phenol of Tyr2225. Introduction of the tricyclic thianthrene side chain (**22**) significantly reduced the cellular mTOR potency, providing a potential upper limit

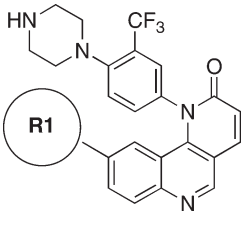

Figure 4. Representative structures of variations of R1.

on the size of the functionality that can be accommodated within the inner hydrophobic pocket. Most of the bicyclic side chains such as benzothiophene (**21**), isoquinoline (**23**), naphthalene (**25**), benzodioxane (**26**), and benzodioxole (**27**) maintained reasonable enzymatic activities, but only those with appropriately placed hydrogen-bond accepting potential (**26**, **27**) displayed good cellular activity. Monocyclic **R1** groups with substitution at the para-position (**20**) possessed activity in the same range as the bicyclic ring systems. The

Table 3. Enzymatic and Cellular Activities Profile of Compounds Varying R1[a]

Entry	R1	mTOR IC_{50}(nM) mTORC1	mTOR IC_{50}(nM) Cellular
19		13.5	40
20		78.9	100
21		93.8	>300
22	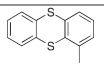	3440	>300
23		33.2	>300
24		662	>300
25		213	>300
26		66.5	150
27		82.6	40
28		45.9	>300
29		214	>300

[a] IC_{50} determinations are the mean of two of independent measurement with standard error of $<20\%$. None of the tested compounds exhibited IC_{50} for inhibition of cellular PI3K activity of less than 300 nM.

dramatic loss of activity observed between compound **24** and **20** may be attributed to the lack of tolerance for α-substitution, which is consistent with the observations made for the compound **10** series.[17] Cumulatively, these data suggest that a combination of hydrophobic and hydrogen bonding interactions are critical for achieving potent cellular inhibition of mTOR and that the quinoline moiety was the preferred core for this pharmacophore. None of the compounds in this series displayed cellular activity against PI3K up to a concentration of 300 nM. A number of discordances were observed between the biochemical and cellular IC_{50} measurements that may be attributed to differential cellular permeability and/or the inability of the biochemical assay to accurately reflect the functionally relevant intracellular mTOR. On the basis of this observation, the cell based IC_{50} was used as a guide for the chemical optimization process.

Following the initial optimization steps, we introduced a variety of side chains to the R2 position while fixing the **R1** side chain as a quinoline (Figure 5 and Table 4). Introducing sulfonyl (**31**) or methylene spacer (**33**) before the piperazine functionality resulted in a loss in mTOR potency. Introducing an *ortho*-methoxy substitution (**32** versus **19**) resulted in a 5-fold loss in cellular mTOR inhibition. Replacement of an **R2** phenyl moiety with small aliphatic side chains (represented by **38**) resulted in inactive compounds. Most compounds that

Table 4. Enzymatic and Cellular Activities Profile of Compounds Varying R2[a]

Entry	R2	mTOR IC_{50}(nM) mTORC1	mTOR IC_{50}(nM) Cellular
19	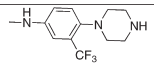	13.5	40
30	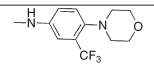	25.8	35
31	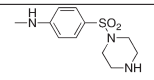	239	>300
32	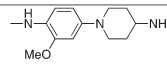	95	200
33	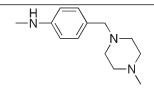	66	250
34	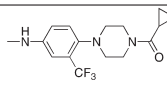	6.84	1
35	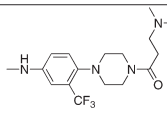	3.6	50
36	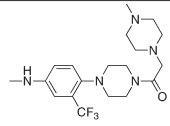	0.57	5
37	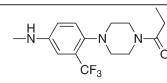	0.29	2
38	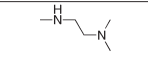	389	>300
39	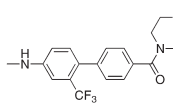	1.26	25
40	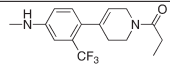	21.4	30
41	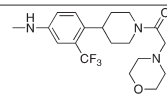	4.25	5

[a] IC_{50} determinations are the mean of two of independent measurement with standard error of $<20\%$. None of the tested compounds exhibited an IC_{50} for inhibition of cellular PI3K activity of less than 300 nM.

retained the *meta*-CF_3 substituted aniline and also those derivatized at the para-position with piperazinyl, phenyl, and piperidinyl groups retained similar or superior potency relative to compound **18**. Introducing a carbonyl moiety in the form of an acetyl group to the piperazine nitrogen (**18** versus **19**) resulted in a 13-fold improvement in cellular potency,

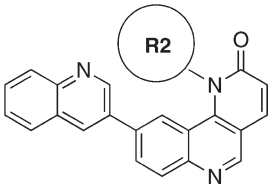

Figure 5. Representative structures of variations of R2.

potentially due to the introduction of a hydrogen bond with Lys2186. (Figure 3) To avoid an 1,4-dianiline moiety that could potentially represent a metabolic liability in compound **18**, several piperazine replacements were explored such as reversed piperidine (**41**), unsaturated piperidine (**40**), or phenyl (**39**) linkage; however, they all resulted in weaker biochemical and cellular mTOR inhibition. Further exploration of the piperazine acyl moiety, which the modeling predicted to be directed toward the solvent area, resulted in the identification of the propyl amide (**37**, named Torin1) as conferring the greatest potency and selectivity. Compound **37** is a picomolar inhibitor of mTORC1 enzymatic activity and single digit nanomolar inhibitor of cellular mTOR activity. Although most compounds in this series have over 100-fold selectivity relative to inhibition of cellular PI3K activity, a more detailed study of **37** revealed that it has more than 800-fold selectivity between mTOR and PI3K.[7]

We next investigated the SAR of the lactam ring using Torin1 as a staring point. The resultant SAR indicated that the rigid six-membered lactam was preferred, as urea, carbamate, and pyrimidinedione analogues lost more than 500-fold activity against the mTORC1 complex (Table 5). Introduction of a methyl group to either the α (**42**) or β position (**43**) of the lactam ring significantly diminished potency in both the biochemical and cellular assays, suggesting these positions make a close contact to the ATP-binding site.

Table 5. Enzymatic and Cellular Activities Profile of Fixed Conformation Compounds[a]

Entry	Structure	mTOR IC_{50}(nM) mTORC1	mTOR IC_{50}(nM) Cellular
37	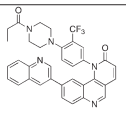	0.29	2
42	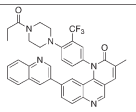	26.6	100
43	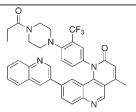	51.9	>300
44	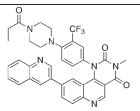	230	300
45	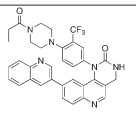	396	>300
46	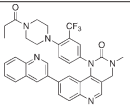	287	100
47	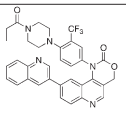	336	>300

[a] IC_{50} determinations are the mean of two of independent measurements with standard error of $<20\%$. **37** has a cellular IC_{50} of 1800 nM for PI3K. None of other compounds exhibited a cellular IC_{50} for PI3K of less than 300 nM.

Kinase Selectivity

Biochemical characterization of **37** at varying ATP concentrations demonstrated that it is an ATP competitive inhibitor of mTOR. The selectivity of **37** was assessed using the KinomeScan methodology across a panel of 442 human kinases at a concentration of 10 μM. Only three kinases displayed tight binding to **37** (Ambit scores of less than 2), and dissociation constants were determined for mTOR, PI3Kα, and PI3Kα (I800L) (Table 6). This analysis revealed that **37** is extremely selective for PIKK family kinases relative to all other serine/threonine and tyrosine kinases. To further investigate these observed binding events, we performed enzymatic assays across most of the known PIKK family kinases using the LanthaScreen technology. This analysis revealed that **37** is very selective relative to other PIKK family kinases with the exception of DNA-PK (Table 7). The activity against DNA-PK was further characterized using a radiometric kinase assay where the compound exhibited an IC_{50} of approximately 1 μM.[7] The origin of the 150-fold discrepancy between the LanthaScreen IC_{50} for DNA-PK versus the radiometric assay is currently unknown.

Pharmacokinetic Data

The pharmacokinetic properties of **37** were next evaluated both in vitro and in vivo. In both human and mouse liver microsome stability studies, **37** was rapidly consumed with a half-life of 4 min (Table 8). The significant difference in human liver microsome metabolism observed in the presence and absence of NADPH indicates a NADPH dependent metabolism mechanism. The in vivo pharmacokinetic parameters of **37** in mice were determined following the intravenous administration of 1 mg/kg, oral administration of 10 mg/kg, or intraperitoneal administration of 10 mg/kg of **37** (Table 9). As expected from the in vitro studies, **37** exhibited a short $T_{1/2}$ of 0.5 h that may partially due to the rapid first-pass metabolism. **37** also exhibited low exposure and limited bioavailability following the oral administration, possibly suggestive of low absorption or high first pass metabolism. The better exposure and much longer half-life achieved following intraperitoneal administration further confirmed the instability of **37** to the liver metabolism.

Pharmacodynamic Data

To assess the pharmacodynamic effects of **37**, mice were treated with a single intraperitoneal dose of 20 mg/kg **37**, and the phosphorylation of S6 at S235/236 and of Akt1 at S473 were measured by Western blot in lysates derived from liver

and lung. **37** suppressed Akt1 phosphorylation at S473, the phosphorylation site of mTORC2, for approximately 2−3 h, after which the phosphorylation gradually returned to baseline levels. Inhibition of S6 at S235/236, an indirect substrate of mTORC1, was more markedly suppressed with complete inhibition of phosphorylation observed up to 6 h in the lung and to greater than 10 h in the liver (Figure 6). These pharmacodynamic studies indicate that despite the poor pharmacological properties of **37**, suppression of both mTORC1 and mTORC2 dependent outputs can be achieved in mice.

Antitumor in Vivo Efficacy

The results from the pharmacodynamic studies encouraged us to investigate whether **37** would inhibit growth in a U87MG xenograft model. U87MG is a PTEN*null* glioblastoma cell line that exhibits strong activation of the PI3K-mTOR-Akt pathway and has been commonly used for xenograft experiments to evaluate the efficacy of PI3K and mTOR kinase inhibitors.[11,28] Because of the relatively poor pharmacokinetic properties, we decided to perform once daily IP dosing of 20 mg/kg of **37**. Continuous dosing for 10 days resulted in greater than 99% inhibition of tumor growth as assessed by caliper measurements. (Figure 7) Upon cessation of drug treatment, the tumors continued to grow, suggesting that **37** treatment is primarily cytostatic and that a significant number of tumor cells remain viable during treatment (data not shown).

Table 6. KinomeScan Profile of **37**[a]

kinase	% control	K_d (nM)	kinase	% control	K_d (nM)
mTOR	0	0.42	PIK3CA(E545K)	0.6	ND
PIK3CA(C420R)	0.7	ND	PIK3CA(I800L)	0	14
PIK3CA	1.3	23	MRCKA	0.65	10000

[a] Compound **37** was profiled at a concentration of 10 μM against a diverse panel of 442 kinases by Ambit Biosciences.

Table 7. LanthaScreen Profile of **37** in Invitrogen Lipid Kinase Panel[a]

kinase	IC_{50} (nM)	kinase	IC_{50} (nM)
PI4K α	> 10000	P110 α/p85α	250
PI4K β	6680	P110δ/P85α	564
PI3K−C2 α	176	P110γ	171
PI3K−C2β	549	DNA-PK	6.34
hVPS34	533	mTOR	4.32

[a] Kinase targets were tested with biochemical enzymatic kinase assays using the SelectScreen Kinase Profiling Service (Life Technologies Corporation, Madison, WI) to determine IC_{50} values as shown in Table 7. The compounds were assayed at 10 concentrations (3-fold serial dilutions starting from 1 μM) at an ATP concentration equal to the ATP $K_{m,app}$ for the assay following the detailed procedures described in the SelectScreen Customer Protocol and Assay Conditions documents located at www.invitrogen.com/kinaseprofiling.

Table 8. Human and Mouse Liver Microsome Stability Data of **37**[a]

species	MR (nmol/min/mg)	$T_{1/2}$ (min)	%*R* at 60 min	%*R* at 60 min (−NADPH)
human	1.30	4	1	69
mouse	1.53	4	0.2	1

[a] Human liver microsome (7 males + 2 females, cat. 452165) and male mouse liver microsomes (cat. 452220) from BD Gentest.

Conclusion

Starting from a quinoline screening "hit" compound **12** discovered using a medium-throughput biochemical mTORC1 assay, a focused medicinal chemistry effort facilitated by molecular modeling and other known PIKK-family inhibitors

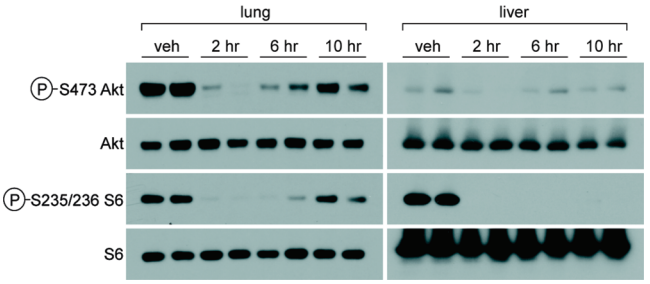

Figure 6. Pharmacodynamic inhibition of Akt S473 and S6 S235/236 phosphorylation in lung and liver of mice treated with a single intraperitoneal dose of 20 mg/kg **37**. Six-week-old male C57BL/6 mice were fasted overnight prior to treatment with **37** as a suspension in 20% *N*-methyl-2-pyrrolidone/40% PEG400/40% water or with vehicle by IP injection. Tissues were collected and analyzed at 2, 6, and 10 h after dosing.

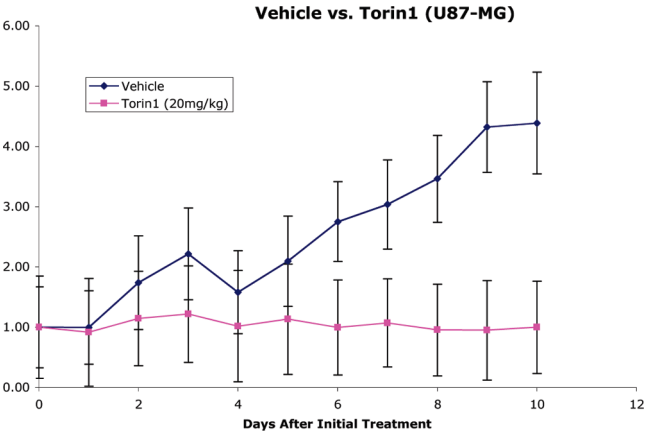

Figure 7. In vivo efficacy of **37** in U87MG xenografts. Mice model was established with six-week-old immunodeficient mice by subcutaneous injection of U87MG cells. **37** as a solution/suspension in vehicle (20% *N*-methyl-2-pyrrolidone, 40% PEG400, and 40% water) or vehicle was delivered by intraperitoneal injection once daily after the tumor reached 1 cm^3 in size and continued for 10 days.

Table 9. Mouse PK Data of **37**[a]

route	C_{max} (ng/mL)	T_{max} (h)	AUC (h·ng/mL)	$T_{1/2}$ (h)	MRT (h)	CL (mL/min/kg)	V_{ss} (L/kg)	*F* (%)
IV	2757	ND	720	0.5	0.43	23.0	0.59	ND
PO	223	0.25	396	0.79	1.51	ND	ND	5.49
IP	5121	0.08	5718	4.52	ND	ND	ND	ND

[a] C57BL/6 male mouse was dosed at 1 mg/kg for the intravenous (IV), 10 mg/kg for the oral (PO), and 10 mg for the intraperitoneal (IP: Swiss albino mice) studies. IV formulation used 10% *N*-methyl pyrrolidone (NMP) and 50% polyethylene glycol (PEG-200) in water. PO formulation used 0.5% w/v NaCMC with 0.1% w/v Tween-80. IP administration formulation was 10% v/v dimethylacetamide (DMA), 20% v/v polyethylene glycol (PEG-200), 20% v/v PG in water.

resulted in the identification of a novel benzonaphthridinone scaffold exemplified by **37**. Compound **37** inhibits phosphorylation of both mTORC1 and mTORC2 at single-digit nanomolar concentrations while exhibiting 800-fold selectivity relative to cellular PI3K inhibitory activity. Compound **37** exhibited a short in vivo half-life and low oral bioavailability but displayed pharmacodynamic inhibition of both mTORC1 and mTORC2 outputs in lung and liver. Compound **37** dosed once a day at 20 mg/kg for 10 days demonstrated efficacy in a U87MG xenograft mouse model. Compound **37** is a valuable tool for investigating mTOR mediated signal pathways and provides a valuable starting point for identification of compounds with improved "drug-like" properties.

Experimental Procedures

Chemistry. All solvents and reagents were used as obtained. ^{1}HNMR spectra were recorded with a Varian Inova 600 NMR spectrometer and referenced to dimethyl sulfoxide. Chemical shifts are expressed in ppm. In the NMR tabulation, s indicates singlet; d, doublet; t, triplet; q, quartet; m, multiplet; and br, broad peak. Mass spectra were measured with Waters Micromass ZQ using an ESI source coupled to a Waters 2525 HPLC system operating in reverse mode with an Waters Sunfire C18 5 μm 4.6 mm $\times$ 50 mm column. Purification of compounds was performed with either a Teledyne ISCO combiflash Rf system or a Waters Micromass ZQ preparative system. The purity of all compounds was $\geq$95%. The purity was analyzed on an above-mentioned Waters LC-MS Symmetry (C18 column, 4.6 mm $\times$ 50 mm, 5 μM) using a gradient of 5−95% acetonitrile in water containing 0.05% trifluoacetic acid (TFA) over 8 min (10 min run time) at a flow rate of 2 mL/min.

General Procedure for the Preparation of Compounds 15−17. To a solution of compound **14** (4,6-dichloroquinoline, 1 equiv) in 1,4-dioxane at room temperature in a sealed tube was added aniline (1 equiv). The resultant solution was heated to 100−120 °C for 4−12 h. After cooling to room temperature, a solution of NaOH (1 N) was added to neutralize the solution followed by dilution with water and extraction with ethyl acetate. After drying with Na_2SO_4, the solvents were removed and the residue was purified by ISCO to furnish compound **13**.

To a solution of compound **13** (1 equiv) in 1,4-dioxane at room temperature was added $PdCl_2(Ph_3P)_2$ (0.1 equiv), *t*-Bu-Xphos (0.1 equiv), Na_2CO_3 (3 equiv, 1 N), and quinoline-3-boronic acid. After degassing, the resultant mixture was heated to 100 °C for 6 h before cooling down to room temperature and filtration through Celite. Upon removal of the solvents, the residue was purified by column chromatography to furnish compounds **15−17**.

1-(4-(4-([3,6′-Biquinolin]-4′-ylamino)-2-(trifluoromethyl)phenyl)-piperazin-1-yl)ethanone (15). Yield 20% overall from **14**. ^{1}H NMR (600 MHz, DMSO-d_6) δ 10.12 (s, 1H), 9.49 (d, J = 2.4 Hz, 1H), 9.05 (d, J = 1.8 Hz, 1H), 8.84 (d, J = 2.4 Hz, 1H), 8.67 (s, 1H), 8.42 (dd, J = 8.4, 2.4 Hz, 1H), 8.26 (dd, J = 8.4, 2.4 Hz, 1H), 8.19 (d, J = 2.4 Hz, 1H), 8.10−8.12 (m, 2H), 7.96 (d, J = 8.4 Hz, 1H), 7.82 (ddd, J = 7.2, 6.6, 1.8 Hz, 1H), 7.69 (ddd, J = 8.4, 7.8, 1.2 Hz, 1H), 7.63 (d, J = 8.4 Hz, 1H), 3.54−3.56 (m, 4H), 2.87 (t, J = 4.8 Hz, 2H), 2.81 (t, J = 4.8 Hz, 2H), 2.04 (s, 3H). MS (ESI): m/z $(M + H)^+$ 542.87.

General Procedure for Compounds 18−42. To a solution of compound **S1** (ethyl 4,6-dichloroquinoline-3-carboxylate, 1 equiv) in 1,4-dioxane at room temperature was added aniline (1 equiv) at room temperature. The reaction mixture was heated to 100 °C for 4 h, followed by cooling to room temperature and the addition of NaOH (1 N) to neutralize the solution. The resultant solution was diluted with water and extracted with ethyl acetate. After removal of the solvents, the residue was purified by flash chromatography to afford compound **S2**.

To a solution of compound **S2** (1 equiv) in THF at 0 °C was added LAH (3 equiv). After 15 min, the solution was warmed to room temperature and stirred for 1−4 h before carefully quenching with methanol and water. Subsequent filtration through Celite furnished crude **S3**, which was used in the next step without further purification.

To a solution of compound **S3** in CH_2Cl_2 (1 equiv) at room temperature was added MnO_2 (10 equiv mass). After 4 h, the reaction mixture was filtered through Celite. The filtrate was concentrated in a sealed tube and dissolved in dry EtOH, after which K_2CO_3 (3 equiv) and triethyl phosphonoacetate (triethyl 2-phosphonopropionate for compound (**42**) were added. The resultant mixture was heated to 100 °C for 12 h before cooling to room temperature. Upon removal of the solvents under vacuum, the residue was diluted with water following by extraction with ethyl acetate. Purification of the residue by column chromatography provided compound **S4**.

To a solution of compound **S4** in 1,4-dioxane at room temperature was added subsequently $PdCl_2(Ph_3P)_2$ (0.1 equiv), *t*-Bu-Xphos (0.1 equiv), Na_2CO_3 (3 equiv, 1 N), and boronic acids or boronate pinacol esters. After degassing, the resultant mixture was heated to 100 °C for 6 h before cooling to room temperature and filtration through Celite. Upon removal of the solvents, the residue was subjected to column purification to furnish the desired compounds (**18−42**).

1-(4-(4-Acetylpiperazin-1-yl)-3-(trifluoromethyl)phenyl)-9-(quinolin-3-yl)benzo[h][1,6]naphthyridin-2(1*H*)-one (18). Yield 15% overall from **S1**. ^{1}H NMR (600 MHz, DMSO-d_6) δ 9.20 (s, 1H), 8.58 (d, J = 1.8 Hz, 1H), 8.34 (d, J = 9.6 Hz, 1H), 8.27 (s, 1H), 8.20 (d, J = 8.4 Hz, 1H), 8.16 (d, J = 7.2 Hz, 1H), 8.04 (d, J = 8.4 Hz, 1H), 7.97−7.98 (m, 2H), 7.79−7.82 (m, 2H), 7.67−7.71 (m, 2H), 7.11 (s, 1H), 6.95 (d, J = 9.0 Hz, 1H), 3.28 (m, 4H), 2.65−2.70 (m, 2H), 2.59 (m, 2H), 1.98 (s, 3H). MS (ESI): m/z $(M + H)^+$ 594.81.

1-(4-(4-Propionylpiperazin-1-yl)-3-(trifluoromethyl)phenyl)-9-(quinolin-3-yl)benzo[h][1,6]naphthyridin-2(1*H*)-one (37). Overall yield 7% from **S1**. ^{1}H NMR (600 MHz, DMSO-d_6) δ 9.19 (s, 1H), 8.58 (d, J = 2.4 Hz, 1H), 8.34 (d, J = 9.6 Hz, 1H), 8.26 (d, J = 1.8 Hz, 1H), 8.19 (d, J = 9.0 Hz, 1H), 8.14 (dd, J = 9.0, 1.8 Hz, 1H), 8.03 (d, J = 9.0 Hz, 1H), 7.96−7.98 (m, 2H), 7.77−7.82 (m, 2H), 7.66−7.70 (m, 2H), 7.09 (d, J = 1.8 Hz, 1H), 6.94 (d, J = 9.6 Hz, 1H), 3.40−3.42 (m, 4H), 2.60−2.65 (m, 4H), 2.28 (q, J = 7.8 Hz, 2H), 0.98 (t, J = 7.8 Hz, 3H). MS (ESI): m/z $(M + H)^+$ 608.23.

General Procedure for the Preparation of Compounds 43−47. Compound **S2** was subjected to Pd mediated coupling with quinoline 3-boronic acid under the conditions mentioned above to furnish compound **S2a** (ethyl 4-(3-(trifluoromethyl)-4-(4-propionylpiperazin-1-yl)phenylamino)-6-(quinolin-3-yl)quinoline-3-carboxylate). Compound **S2a** was dissolved in a mixture of MeOH/H_2O (1:1) and treated with NaOH (1 N, 5 equiv) at room temperature. The reaction mixture was then stirred overnight. The pH of the solution was adjusted to 4, followed by extraction with ethyl acetate to afford the crude carboxylic acid **S2b**. Acid **S2b** (1 equiv) was dissolved in THF at room temperature and treated with triphosgene (0.4 equiv). After 2 h, methylamine (2 equiv) was added and the resulting mixture was heated at 40 °C for 1 h before quenching with saturated Na_2CO_3. Extraction with ethyl acetate followed by column chromatography afforded compound **44**.

To a solution of compound **S2b** in THF was added methyl methoxyamine (2 equiv), Et_3N (3 equiv), and HATU (2 equiv). The resultant solution was stirred at room temperature for 4 h before extraction with ethyl acetate. Column purification afforded Weinreb amide **S2c**, which was then dissolved in THF and treated with methyl magnesium bromide (3 equiv) at room temperature. The resulting solution was stirred for 4 h before quenching with satd Na_2CO_3. Column chromatography afforded methyl ketone **S2d**, which was further elaborated to compound **43** in the same fashion as the synthesis of compound **18**.

To a solution of compound **S3** (1 equiv) in THF at room temperature was added triphosgene (0.4 equiv). The resultant

solution was stirred at room temperature for 2 h before it was quenched with satd Na_2CO_3. Column chromatography afforded compound **47**.

To a solution of compound **S3** in CH_2Cl_2 (1 equiv) at room temperature was added MnO_2 (10 equiv mass). The mixture was stirred for 4 h before being filtered through Celite. The filtrate was concentrated, dissolved in THF, and treated with methyl amine (2 equiv for compound **46**) or 2,4-dimethoxylbenzylamine (2 equiv for compound **45**), $NaBH(OAc)_3$ (5 equiv), and AcOH (1 drop) at room temperature. The reaction mixture was stirred for 4 h before it was quenched with satd Na_2CO_3. After compound purification, the corresponding product was subjected to the same procedure as in the preparation of compound **43** to afford compounds **45** and **46**.

Characterization of in Vitro Biochemical Activity with the mTORC1 Complex. Human mTORC1 complex was obtained as previously described.[7,29] In vitro mTORC1 activity was assayed using the Lanthascreen time-resolved FRET assay (Invitrogen). Briefly, mTORC1 (0.1 μg each) was incubated with serially diluted inhibitors (3-fold, 11 points) for 30 min in 5 μL of kinase buffer (25 mM HEPES, pH 7.4, 10 mM $MgCl_2$, 4 mM $MnCl_2$, 50 mM KCl) in a 384-well low-volume plate (Corning). The kinase reaction was initiated by the addition of an equal volume of kinase buffer containing 0.8 μM GFP-labeled 4E-BP1 and 100 μM ATP at room temperature and, after 1 h, the reaction was stopped with 10 μL of solution containing 20 mM EDTA and 4 nM Tb-labeled antiphospho 4E-BP1 (T46) antibody. After incubation for 30 min, the FRET signal between Tb and GFP within the immune complex was read using an Envision plate reader (PerkinElmer). Each data point was duplicated and IC_{50} values were calculated using Prism4 software (GraphPad).

mTOR and PI3K Cellular Assays. Cellular IC_{50} values for mTOR were determined using $p53^{-/-}$ MEFs. Cells were treated with vehicle or increasing concentrations of compound for 1 h and then lysed. Phosphorylation of S6K1 Thr-389 was monitored by immunoblotting using a phospho-specific antibody. Meanwhile, cellular IC_{50} values for PI3Ka were determined based on phosphorylation of Akt Thr-308 in $p53^{-/-}$/$mLST8^{-/-}$ MEFs or human PC3 cells expressing the S473D mutant of Akt1 as previously described.[7]

Ambit in Vitro KinomeScan Kinase Selectivity Profile. 37 was profiled at a concentration of 10 μM against a diverse panel of 442 kinases by Ambit Biosciences. Scores for primary screen hits are reported as a percent of the DMSO control (% control). For kinases where no score is shown, no measurable binding was detected. The lower the score, the lower the K_d is likely to be, such that scores of zero represent strong hits. Scores are related to the probability of a hit but are not strictly an affinity measurement. At a screening concentration of 10 μM, a score of less than 10% implies that the false positive probability is less than 20% and the K_d is most likely less than 1 μM. A score between 1% and 10% implies that the false positive probability is less than 10%, although it is difficult to assign a quantitative affinity from a single-point primary screen. A score of less than 1% implies that the false positive probability is less than 5% and the K_d is most likely less than 1 μM.

In Vivo Pharmacokinetic Studies. The study was performed at the Sai Advantium Pharma Limited Company (India) with male Swiss albino mice following single intravenous bolus and oral administration. A group of 18 male mice were divided into two groups (group 1, IV; group 2, PO), with each group comprised of nine mice. Animals in group 1 were dosed intravenously via the tail vein at 1 mg/kg of **37** solution (10% v/v *N*-methyl pyrrolidone and 50% v/v polyethylene glycol-200 in normal saline). Group 2 animals were dosed orally at 10 mg/kg with a suspension formulation (0.5% w/v Na CMC with 0.1% v/v Tween-80 in water) of **37**. Blood samples were collected at 0, 0.08 (for IV only), 0.25, 0.5, 1, 2, 4, 6 (For PO only), 8, 12, and 24 h for the IV and PO groups. IP experiment was one with Swiss albino mice using formulation as 10% v/v dimethylacetamide(DMA), 20% v/v polyethylene glycol(PEG-200), 20% v/v PG in water. The blood samples were collected from sets of three mice at each time point in labeled microcentrifuge tubes containing K2EDTA as an anticoagulant. Plasma samples were separated by centrifugation and stored below −70 °C until bioanalysis. All samples were processed for analysis by precipitation using acetonitrile and analyzed with a partially validated LC/MS/MS method (LLOQ, 1.138 ng/mL). Pharmacokinetic parameters were calculated using the noncompartmental analysis tool of WinNonlin Enterprise software (version 5.2).

Antitumor (U87MG model) Efficacy Studies. Immunodeficient mice (NCR nude, nu/nu; Taconic Laboratories) were maintained in a pathogen-free facility and were given autoclaved food and water ad libitum. U87-MG glioblastoma cells were xenografted into six-week-old immunodeficient mice. Briefly, 2×10^6 U87MG cells were resuspended in 100 μL of media that had been premixed with Matrigel and was injected subcutaneously in the upper flank region of mice that had been anaesthetized with isoflurane. Tumors were allowed to grow to 1 cm^3 in size, and the animals were randomized into two treatment groups: vehicle and **37**. For **37** injections, **37** powder was first dissolved at 25 mg/mL in 100% *N*-methyl-2-pyrrolidone and subsequently diluted 1:4 with sterile 50% PEG400 to a final concentration of 5 mg/mL **37**. Vehicle or **37** was delivered by IP injection at the indicated dosage once daily. Tumors were measured with calipers in two dimensions every other day. Tumor volumes were estimated with the formula: volume = $(2a \times b)/2$, where a = short and b = long tumor axes, respectively, in millimeters. All animal studies were performed according to the official guidelines from the MIT Committee on Animal Care and the American Association of Laboratory Animal Care.

In Vivo Pharmacodynamic Studies. For pharmacodynamic experiments, **37** powder was first dissolved at 25 mg/mL in 100% *N*-methyl-2-pyrrolidone and then diluted 1:4 with sterile 50% PEG400 prior to injection. Six-week old male C57BL/6 mice were fasted overnight prior to drug treatment. The mice were treated with vehicle (for 10 h) or **37** (20 mg/kg for 2, 6, or 10 h) by IP injection and then re-fed 1 h prior to sacrifice (CO_2 asphyxiation). Tissues were collected and frozen on dry ice. The frozen tissue was thawed on ice and lysed by sonication in tissue lysis buffer (50 mM HEPES, pH 7.4, 40 mM NaCL, 2 mM EDTA, 1.5 mM sodium orthovanadate, 50 mM sodium fluoride, 10 mM sodium pyrophosphate, 10 mM sodium β-glycerophosphate, 0.1% SDS, 1.0% sodium deoxycholate, and 1.0% Triton, supplemented with protease inhibitor cocktail tablets (Roche)). The concentration of clear lysate was measured using the Bradford assay and samples were subsequently normalized by protein content and analyzed by SDS-PAGE and immunoblotting.

Molecular Modeling. An mTOR homology model was built with Modeler(9v6) based on a published PI3Kγ crystal structure complexed with GDC-0941 (PDB: 3DBS). **37** was docked into the model with Pair fitting, followed by energy minimization with Discovery Studio II.

Acknowledgment. We thank Life Technologies Corporation, SelectScreen Kinase Profiling Service for performing enzymatic biochemical kinase profiling. We also thank Ambit Bioscience for performing KinomeScan profiling and Dr. David Waller (Dana Farber Cancer Institute) for the useful proofreading.

Supporting Information Available: Spectral data of **16**−**17**, **19**−**36**, **38**−**47**. This material is available free of charge via the Internet at http://pubs.acs.org.

References

(1) Guertin, D. A.; Sabatini, D. M. Defining the role of mTOR in cancer. *Cancer Cell* **2007**, *12*, 9–22.

(2) Abraham, R. T. PI 3-kinase related kinases: "big" players in stress-induced signaling pathways. *DNA Repair* **2004**, *3*, 883–887.
(3) Shor, B.; Gibbons, J, J.; Abraham, R, T.; Yu, K. Targeting mTOR globally in cancer: thinking beyond rapamycin. *Cell Cycle* **2009**, *8*, 3831–3837.
(4) Liu, Q.; Thoreen, C.; Wang, J.; Sabatini, D.; Gray, N. S. mTOR mediated anti-cancer drug discovery. *Drug Discovery Today: Ther. Strategies* **2009**, *6*, 47–55.
(5) Sarbassov, D. D.; Ali, S. M.; Sengupta, S.; Sheen, J. H.; Hsu, P. P.; Bagley, A. F.; Markhard, A. L.; Sabatini, D. M. Prolonged rapamycin treatment inhibits mTORC2 assembly and Akt/PKB. *Mol. Cell* **2006**, *22*, 159–168.
(6) Lane, H. A.; Breuleux, M. Optimal targeting of the mTORC1 kinase in human cancer. *Curr. Opin. Cell. Biol.* **2009**, *21*, 219–229.
(7) Thoreen, C. C.; Kang, S. A.; Chang, J.; Liu, Q.; Zhang, J.; Gao, Y; Reichling, L. J.; Sim, T.; Sabatini, D. M.; Gray, N. S. An ATP-Competitive Mammalian Target of Rapamycin Inhibitor Reveals Rapamycin-Resistant Functions of mTORC1. *J. Biol. Chem.* **2009**, *284*, 8023–8032.
(8) Feldman, M. E.; Apsel, B.; Uotila, A.; Loewith, R.; Kinght, Z. A.; Ruggero, D.; Shokat, K. M. Active-Site Inhibitors of mTOR Target Rapamycin-Resistant Outputs of mTORC1 and mTORC2. *PLoS Biol.* **2009**, *7*, 371–383.
(9) Garcia-martinez, J. M.; Moran, J.; Clarke, R. G.; Gray, A.; Cosulich, S. C.; Chresta, C. M.; Alessi, D. R. Ku-0063794 is a specific inhibitor of the mammalian target of rapamycin (mTOR). *Biochem. J.* **2009**, *421*, 29–42.
(10) Yu, K.; Toral-Barza, L.; Shi, C.; Zhang, W.; Lucas, J.; Shor, B.; Kim, J.; Verheijen, J.; Curran, K.; Malwitz, D. J.; Cole, D. C.; Ellingboe, J.; Ayral-kaloustian, S.; Mansour, T., S.; Gibbons, J. J.; Abraham, R. T.; Nowak, P.; Zask, A. Biochemical, Cellular, and in Vivo Activity of Novel ATP-Competitive and Selective Inhibitors of the Mammalian Target of Rapamycin. *Cancer. Res.* **2009**, *69*, 6232–6240.
(11) Barr, S.; Russo, S.; Buck, E.; Epstein, D.; Miglarese, M. Co-targeting mTOR and IGF-1R/IR results in synergistic activity against a broad array of tumor cell lines, independent of KRAS mutation status. AACR 101st Annual Meeting, Washington, DC, April, 2010, p 1632.
(12) Chresta, C. M.; Davies, B. R.; Hickson, I.; Harding, T.; Cosulich, S.; Critchlow, S. E.; Vincent, J. P.; Ellson, R.; Jones, D.; Sini, P.; James, D.; Howard, Z.; Dudley, P.; Hughes, G.; Smith, L.; Maguire, S.; Hummersone, M.; Malagu, K.; Menear, K.; Jenkins, R.; Jacobsen, M.; Smith, G. C. M.; Guichard, S.; Pass, M. AZD8055 Is a Potent, Selective, and Orally Bioavailable ATP-Competitive Mammalian Target of Rapamycin Kinase Inhibitor with in Vitro and in Vivo Antitumor Activity. *Cancer Res.* **2010**, *70*, 288–298.
(13) Menear, K. A.; Gomez, S.; Malagu, K.; Bailey, C.; Blackburn, K.; Cockcroft, X.; Ewen, S.; Fundo, A.; Gall, A. L.; Hermann, G.; Sebastian, L.; Sunose, M; Presnot, T.; Torode, E.; Hickson, I.; Martin, N. M.; Smith, G. C. M.; Pike, K. G. Identification and optimization of novel and selective small molecular weight kinase inhibitors of mTOR. *Bioorg. Med. Chem. Lett.* **2009**, *19*, 5898–5901.
(14) Richard, D. J.; Verheijen, J. C.; Curran, K.; Kaplan, J.; Toral-Barza, L.; Hollander, I.; Lucas, J.; Yu, K.; Zask, A. Incorporation of water-solubilizing groups in pyrazolopyrimidine mTOR inhibitors: discovery of highly potent and selective analogs with improved human microsomal stability. *Bioorg. Med. Chem. Lett.* **2009**, *19*, 6830–6835.
(15) Park, S.; Chapuis, N.; Bardet, V.; Tamburini, J.; Gallay, N.; Willems, L.; Knight, Z. A.; Shokat, K. M.; Azar, N.; Viguie, F.; Ifrah, N.; Dreyfus, F; Mayeux, P.; Lacombe, C.; Bouscary, D. PI-103, a dual inhibitor of class IA phosphatidylinositide 3-kinase and mTOR, has antileukemic activity in AML. *Leukemia* **2008**, *22*, 1698–1706.
(16) Serra, V.; Markman, B.; Scaltriti, M.; Eichhorn, P. J. A.; Valero, V.; Guzman, M.; Botero, M. L.; Llonch, E.; Atzori, F.; Cosimo, S. D.; Maira, M.; Garcia-Echeverria, C.; Parra, J. L.; Arribas, J.; Baselga, J. NVP-BEZ235, a Dual PI3K/mTOR Inhibitor, Prevents PI3K Signaling and Inhibits the Growth of Cancer Cells with Activating PI3K Mutations. *Cancer Res.* **2008**, *68*, 8022–8030.
(17) Sutherlin, D. P.; Sampath, D; Berry, M.; Castanedo, G.; Chang, Z.; Chuckowree, I.; Doston, J.; Folkes, A.; Freidman, L.; Goldsmith, R.; Heffron, T.; Lee, L.; Lesnick, J.; Lewis, C.; Mathieu, S.; Nonomiya, J.; Olivero, A.; Pang, J.; Prior, W. W.; Salphati, L.; Sideris, S.; Tian, Q.; Tsui, V.; Wan, N.; Wang, S.; Wiesmann, C.; Wong, S.; Zhu, B. Discovery of (Thienopyrimidin-2-yl)aminopyrimidines as Potent, Selective, and Orally Available Pan-PI3-Kinase and Dual Pan-PI3-Kinase/mTOR Inhibitors for the Treatment of Cancer. *J. Med. Chem.* **2010**, *53*, 1086–1097.
(18) Knight, S. D.; Adams, N. D.; Burgess, J. L.; Chaudhari, A. M.; Darcy, M. G.; Donatelli, C. A.; Luengo, J. I.; Newlander, K. A.; Parrish, C. A.; Ridgers, L.; Sarpong, M. A.; Schmidt, S. J.; Van Aller, G. S.; Carson, J. D.; Diamond, M. A.; Elkins, P. A.; Gardiner, C. M.; Garver, E.; Gilbert, S. A.; Gontarek, R. R.; Jackson, J. R.; Kershner, K. L.; Luo, L.; Raha, K.; Sherk, C. S.; Sung, C.; Sutton, D.; Tummino, P. J.; Wegrzyn, R. J.; Auger, K. R.; Dhanak, D. Discovery of GSK2126458, a Highly Potent Inhibitor of PI3K and the Mammalian Target of Rapamycin. *ACS Med. Chem. Lett.* **2010**, *1*, 39–43.
(19) Sancak, Y.; Peterson, T. R.; Shaul, Y. D.; Lindquist, R. A.; Thoreen, C. C.; Peled, L. B.; Sabatini, D. M. The Rag GTPases Bind Raptor and Mediate Amino Acid Signaling to mTORC1. *Science* **2008**, *320*, 1496–1501.
(20) Ding, S.; Gray, N. S.; Wu, X.; Ding, Q.; Schultz, P. G. A combinatorial scaffold approach toward kinase-directed heterocycle libraries. *J. Am. Chem. Soc.* **2002**, *124*, 1594–1596.
(21) Rabindran, S. K.; Discafani, C. M.; Rosfjord., E. C.; Baxter, M; Floyd, M. B.; Golas, J.; Hallett, W. A.; Johnson, B. D.; Nilakantan, R.; Overbeek, E.; Reich, M. F.; Shen, R.; Shi, X.; Tsou, H. R.; Wang, Y. F.; Wissner, A. Antitumor activity of HKI-272, an orally active, irreversible inhibitor of the HER-2 tyrosine kinase. *Cancer Res.* **2004**, *64*, 3958–3965.
(22) Xia, W.; Mullin, R. J.; Keith, B. R.; Liu, L. H.; Ma, H.; Rusanak, D. W.; Owens, G.; Alligood, K. J.; Spector, N. L. Anti-tumor activity of GW572016: a dual tyrosine kinase inhibitor blocks EGF activation of EGFR/erbB2 and downstream Erk1/2 and AKT pathways. *Oncogene* **2002**, *21*, 6255–6263.
(23) Aoki, M.; Batista, O.; Bellacosa, A.; Tsichlis, P.; Vogt, P. K. The Akt kinase: molecular determinants of oncogenicity. *Proc. Natl. Acad. Sci. U.S.A.* **1998**, *95*, 14950–14955.
(24) (a) Stowasser, F.; Banziger, M.; Garad, S. D. Salts and crystalline forms of 2-methyl-2-[4-(3-methyl-2-oxo-8-quinolin-3-yl-2,3-dihydroimidazo[4,5-*c*]quinolin-1-yl)-phenyl]propionitrile. PCT. Int. Appl. WO2008064093, 2008. (b) Garcia-Echeverria, C.; Capraro, H.; Furet, P. 1H-imidazo[4,5-*c*]quinoline derivatives in the treatment of protein kinase dependent diseases. PCT. Int. Appl. WO03097641, 2003.
(25) (a) Stauffer, F.; Maira, S. M.; Furet, P.; Garcia-Echeverria, C. Imidazo[4,5-*c*]quinolines as inhibitors of the PI3K/PKB-pathway. *Bioorg. Med. Chem. Let.* **2008**, *18*, 1027–1030. (b) Stauffer, F.; Holzer, P.; Garcia-Echeverria, C. Blocking the PI3K/PKB pathway in tumor cells.. *Curr. Med. Chem.—Anti-Cancer Agents.* **2005**, *5*, 449–462.
(26) (a) Rewcastle, G. W.; Palmer, B. D.; Bridges, A. J.; Showalter, H. D. H.; Sun, L.; Nelson, J.; McMichael, A.; Kraker, A. J.; Fry, D. W.; Denny, W. A. Tyrosine Kinase Inhibitors. 9. Synthesis and Evaluation of Fused Tricyclic Quinazoline Analogues as ATP Site Inhibitors of the Tyrosine Kinase Activity of the Epidermal Growth Factor Receptor. *J. Med. Chem.* **1996**, *39*, 918–928. (b) Gazit, A.; Yee, K.; Uecker, A.; Bohmer, F. D.; Sjoblom, T.; Ostman, A.; Waltenberger, J.; Golomb, G.; Banai, S.; Heinrich, M. C.; Levitzki, A. Tricyclic Quinoxalines as Potent Kinase Inhibitors of PDGFR Kinase, Flt3 and Kit. *Bioorg. Med. Chem.* **2003**, *11*, 2007–2018. (c) Coumar, M. S.; Wu, J.; Leou, J.; Tan, U.; Chang, C.; Chang, T.; Lin, W.; Hsu, J. T.; Chao, Y.; Wu, S.; Hsieh, H. Aurora kinase A inhibitors: identification, SAR exploration and molecular modeling of 6,7-dihydro-4H-pyrazolo-[1,5-a]pyrrolo[3,4-d]pyrimidine-5,8-dione scaffold. *Bioorg. Med. Chem. Lett.* **2008**, *18*, 1623–1627. (d) Moro, S.; Varano, F.; Cozza, G.; Pagano, M. A.; Zagotto, G.; Chilin, A.; Guiotto, A.; Catarzi, D.; Calotta, V.; Pinna, L. A.; Meggio, F. Pyrazoloquinazoline Tricyclic System as Novel Scaffold to Design New Kinase CK2 inhibitors. *Lett. Drug Des. Discovery* **2006**, *3*, 281–284. (e) Kempson, J.; Spergel, S. H.; Guo, J.; Quesnelle, C.; Gill, P.; Belanger, D.; Dyckman, A. J.; Li, T.; Watterson, S. H.; Langevine, C. M.; Das, J.; Moquin, R. V.; Furch, J. A.; Marinier, A.; Dodier, M.; Martel, A.; Nirschl, D.; Kirk, K. V.; Burke, J. R.; Pattoli, M. A.; Gillooly, K.; McIntyre, K. W.; Chen, L.; Yang, Z.; Marathe, P. H.; Wang-Iverson, D.; Dodd, H. H.; McKinnon, M.; Barrish, J. C.; Pitts, W. J. Novel Tricyclic Inhibitors of IKB Kinase. *J. Med. Chem.* **2009**, *52*, 1994–2005.
(27) Maira, S.; Stauffer, F.; Brueggen, J.; Furet, P.; Schnell, C.; Fritsch, C.; Brachmann, S.; Chene, P.; Pover, A. D.; Schoemaker, K.; Fabbro, D.; Gabriel, D.; Simonen, M.; Murphy, L.; Finan, P.; Sellers, W.; Garcia-Echeverria, C. G. Identification and characterization of NVP-BEZ235, a new orally available dual phosphatidylinositol 3-kinase/mammalian target of rapamycin inhibitor with potent in vivo antitumor activity. *Mol. Cancer Ther.* **2008**, *7*, 1851–1863.
(28) Knight, Z. A.; Gonzalez, B.; Feldman, M.; Zunder, E. R.; Goldenberg, D. D.; Williams, O.; Loewith, R.; Stokoe, D.; Balla, A.; Toth, B.; Balla, T.; Weiss, W.; Williams, R. L.; Shokat, K. M. A Pharmacological Map of the PI3-K Family Defines a Role for p110α in Insulin Signaling. *Cell* **2006**, *125*, 733–747.
(29) Yip, C. K.; Murata, K.; Walz, T.; Sabatini, D. M.; Kang, S. A. Structure of the Human mTOR Complex I and Its Implications for Rapamycin Inhibition. *Mol. Cell* **2010**, *5*, 768–774.